Received: *September 7, 1998*, Accepted: *October 12, 1998*

Towards a lattice determination of the $B^*B\pi$ coupling

UKQCD Collaboration

Giulia M. de Divitiis, Luigi Del Debbio, Massimo Di Pierro and Jonathan M. Flynn

Dept. of Physics and Astronomy, Univ. of Southampton, Southampton SO17 1BJ, UK
E-mail: giulia@hep.phys.soton.ac.uk, ldd@hep.phys.soton.ac.uk, mdp@hep.phys.soton.ac.uk, j.flynn@hep.phys.soton.ac.uk

Chris Michael and Janne Peisa*

DAMTP, Univ. of Liverpool, Liverpool L69 3BX, UK
E-mail: cmi@liv.ac.uk, J.J.Peisa@swansea.ac.uk

Abstract: The coupling $g_{B^*B\pi}$ is related to the form factor at zero momentum of the axial current between B^*- and B-states. This form factor is evaluated on the lattice using static heavy quarks and light quark propagators determined by a stochastic inversion of the fermionic bilinear. The $g_{B^*B\pi}$ coupling is related to the coupling g between heavy mesons and low-momentum pions in the effective heavy meson chiral lagrangian. The coupling of the effective theory can therefore be computed by numerical simulations. We find the value $g = 0.42(4)(8)$. Besides its theoretical interest, the phenomenological implications of such a determination are discussed.

Keywords: Lattice Gauge Field Theories, B-Physics.

*Present address: Dept. of Physics, Univ. of Wales Swansea, Singleton Park, Swansea SA2 8PP, UK.

Contents

1. Introduction

The precise determination of the Cabibbo-Kobayashi-Maskawa (CKM) matrix will provide a stringent consistency test of the Standard Model (SM), together with new handles to understand CP violation and search for hints of new physics. As far as the heavy flavour sector is concerned, a large amount of experimental data is expected from B-factories and CLEO in the near future. Non-perturbative QCD effects are the main source of systematic error in the extraction of fundamental parameters from experimental data: reliable results depend on some way to tame the large-distance dynamics.

Lattice simulations provide a powerful tool to investigate non-perturbative dynamics from first principles, but systematic errors are introduced by the finite lattice spacing and the restricted range of quark masses which may be simulated. A different approach is based on exploiting exact or approximate symmetries of the theory to write effective lagrangians describing the large distance behaviour in terms of effective meson fields. The chiral symmetry of strong interactions in the limit where $m_q \to 0$ constrains the terms appearing in the chiral lagrangian. The couplings in this lagrangian are phenomenological inputs, which need to be taken either from experimental data or from some other source. On the other hand, when the quark masses tend towards infinity, heavy quark effective theory (HQET) has proved to be a powerful tool to study heavy-flavour physics. However, HQET is less powerful when applied to heavy-to-light transitions, like $B \to \pi$, where the normalisation of matrix elements is not fixed by the symmetry. A combination of these two symmetries has been used in recent years to develop the heavy meson chiral lagrangian (HMχ), describing the interactions of low-momentum pions with mesons containing a single heavy quark [1] (for reviews see [2, 3]).

The definitions and notations used throughout this paper are conveniently introduced by a succint description of the building blocks of this effective theory.

For the heavy degrees of freedom, heavy quark symmetry predicts that the wave function of a heavy meson is independent of the flavour and spin of the heavy quark, leading to a covariant representation of heavy mesonic states [4]. The angular momentum j and the parity P of the light degrees of freedom determine a degenerate doublet of states with spin–parity $J^P = (j \pm 1/2)^P$. The pseudoscalar and vector mesons (e.g. B and B^*) correspond to the $j = 1/2$ case and are described by a 4×4 Dirac matrix H with two spinor indices, one for the heavy quark and one for the light degrees of freedom. In terms of the effective meson fields:

$$H = \frac{1 + \not{v}}{2} \left[B^*_\mu \gamma^\mu - B \gamma_5 \right] , \qquad \overline{H} = \gamma^0 H^\dagger \gamma^0 \, , \tag{1.1}$$

where v is the velocity of the meson and B and B^* are the annihilation operators for particles containing a b quark in the initial state. These meson fields are used in the effective lagrangian to describe the heavy mesons. The light mesons are treated as an octet of pseudo-Goldstone bosons according to the usual chiral lagrangian formalism. At low-momentum the strong interactions of B and B^* mesons with light pseudoscalars are described by the couplings in the effective lagrangian; the lowest order interaction is given by [1, 3]

$$\mathcal{L}^{\rm int}_{\rm HM\chi} = g \, {\rm Tr}(\overline{H}_a H_b \mathcal{A}^{ba}_\mu \gamma^\mu \gamma^5) \, , \tag{1.2}$$

where

$$\mathcal{A}_\mu = \frac{i}{2} (\xi^\dagger \partial^\mu \xi - \xi \partial^\mu \xi^\dagger) \tag{1.3}$$

with $\xi = \exp(i\mathcal{M}/f)$. $\mathcal{M}$ is a 3×3 matrix of π, η and K fields

$$\mathcal{M} = \begin{pmatrix} \pi^0/\sqrt{2} + \eta/\sqrt{6} & \pi^+ & K^+ \\ \pi^- & -\pi^0/\sqrt{2} + \eta/\sqrt{6} & K^0 \\ K^- & \bar{K}^0 & -\sqrt{2/3}\eta \end{pmatrix} \tag{1.4}$$

and the trace is over Dirac indices. At tree level f can be set equal to f_π (the definition of the decay constant used here sets $f_\pi = 132\,{\rm MeV}$). The roman indices a and b denote light quark flavour and repeated indices are summed over $1, 2, 3$. The expansion of $\mathcal{A}$ in terms of pion fields begins with a linear term,

$$\mathcal{A}_\mu = -\frac{1}{f} \partial_\mu \mathcal{M} + \cdots \tag{1.5}$$

The coupling g in eq. (1.2) can easily be related to the $B^* B \pi$ coupling defined as [5, 6]

$$\langle B^0(p) \pi^+(q) | B^{*+}(p') \rangle = -g_{B^* B \pi}(q^2) q_\mu \eta^\mu(p') \, (2\pi)^4 \, \delta(p' - p - q) \, , \tag{1.6}$$

where η^μ is the polarisation vector of the B^* and the physical states are relativistically normalised:

$$\langle B(p)|B(p')\rangle = 2p^0(2\pi)^3\delta^{(3)}(\mathbf{p}-\mathbf{p}')\,. \tag{1.7}$$

The physical coupling $g_{B^*B\pi}$ is given by the value of the above form factor for an on-shell pion:

$$g_{B^*B\pi} = \lim_{q^2\to m_\pi^2} g_{B^*B\pi}(q^2)\,. \tag{1.8}$$

At tree level in the heavy meson chiral lagrangian, the above matrix element is

$$\langle B^0(p)\pi^+(q)|B^{*+}(p')\rangle = -\frac{2m_B}{f_\pi}\, g\, q_\mu\eta^\mu(p')\,(2\pi)^4\,\delta(p'-p-q)\,, \tag{1.9}$$

which therefore yields

$$g_{B^*B\pi} = \frac{2m_B}{f_\pi} g\,. \tag{1.10}$$

As a result, g and $g_{B^*B\pi}$ are considered as equivalent throughout this paper. The above relation can be extended to take into account higher-order terms in the HMχ lagrangian [7, 8, 9].

Starting from eq. (1.6) and performing an LSZ reduction of the pion field, the coupling g is related to the form factor at zero momentum-transfer of the axial current between hadronic states. Such a relation is the analog, in the $B\pi$ system, of the Goldberger-Treiman relation, relating the nucleon electromagnetic form factor to the nucleon-nucleon-pion coupling. An important consequence of the Goldberger-Treiman relation, for our purposes, is that it allows a numerical evaluation of the $g_{B^*B\pi}$ coupling, as the form factors of the axial current can be evaluated by a lattice simulation. The details of the pion reduction are presented in sect. 2.

The interest of such a computation is twofold. From a theoretical point-of-view, it is interesting *per se* to be able to fix, from lattice QCD, the coupling appearing in the heavy meson chiral lagrangian. On the other hand, it is important to stress that this determination also has phenomenological motivations. Assuming vector dominance in the $B\to\pi l\nu$ decay, the coupling $g_{B^*B\pi}$ fixes the normalisation of the form factors used to parametrise the matrix element of the weak vector current, $V^\mu = \bar u\gamma^\mu b$, between hadronic states. Defining the form factors by

$$\begin{aligned}\langle\pi^+(p')|V^\mu|\bar B(p)\rangle &= f_1(q^2)(p+p'-\frac{m_B^2-m_\pi^2}{q^2}q)^\mu + f_0(q^2)\frac{m_B^2-m_\pi^2}{q^2}q^\mu = \\ &= f_+(q^2)(p+p')^\mu + f_-(q^2)q^\mu\,,\end{aligned} \tag{1.11}$$

where $q=p-p'$ is the transferred momentum, the contribution from the B^* channel is easily evaluated:

$$f_1(q^2) = \frac{g_{B^*B\pi}}{2f_{B^*}}\frac{1}{1-q^2/m_{B^*}^2}\,. \tag{1.12}$$

The normalisation of the form factor therefore depends on the $B^*B\pi$ coupling and the decay constant of the vector meson, defined as

$$\langle 0|V^\mu|\bar{B}^*(p)\rangle = i\frac{m_{B^*}^2}{f_{B^*}}\eta^\mu(p)\,. \tag{1.13}$$

Heavy quark symmetry and chiral symmetry justify this pole form for f_1 when q^2 is close to $q^2_{\rm max} = (m_B - m_\pi)^2$ [1, 7, 8, 9, 10, 11]. For q^2 far from $q^2_{\rm max}$, the pole form may be taken as a phenomenological ansatz. However, we note that the functional dependence of the form factor in eq. (1.12) cannot be simultaneously consistent with heavy quark symmetry at large q^2, which demands that $f_1(q^2_{\rm max}) \sim m_B^{1/2}$ and the light-cone sum rule scaling relation at $q^2 = 0$, which states $f_1(q^2{=}0) \sim m_B^{-3/2}$ [12].[1] Nonetheless, by fitting lattice results, which are available in the high q^2 region where the pole form is justified, we can determine the parameters in eq. (1.12).

It is interesting to remark that the interplay of the effective lagrangian approach and lattice simulations provides another determination of the form factors for the heavy-to-light B decays and therefore sheds further light on the theoretical determination of the non-perturbative effects mentioned at the beginning. This result can be compared with direct computations of the same quantities obtained by fitting lattice data [14], using unitarity bounds [15] and sum rules [6, 16].

In the work described here, the matrix element of the light quark axial current between the heavy mesons is computed in a quenched lattice simulation of QCD in the static heavy quark limit, using stochastic methods to compute the desired light quark propagators, as described in sect. 3. The discussion of systematic errors is an important issue in any lattice calculation and plays a crucial part in estimating the error on the final result. In this respect, it is important to stress here that we are presenting an exploratory study. Our main concern is therefore to test the possibility of extracting the coupling defined above, rather than presenting its best lattice determination. Such a task would require a more extensive simulation and is left for further studies.

Renormalisation constants are needed in order to connect lattice results with continuum physical observables. Those relevant for the action and the quantities considered in this paper are summarised in sect. 4.

The best estimate we obtain for g is

$$g = 0.42(4)(8)\,. \tag{1.14}$$

The phenomenological implications of this result are discussed in sect 5.

[1] Light-cone sum rules have also been applied at large q^2 and reproduce the $m_B^{1/2}$ scaling behaviour of f_1 as demanded by heavy quark symmetry [13].

2. Pion reduction

An LSZ reduction of the pion in the definition of $g_{B^*B\pi}$, eq. (1.6), yields

$$\langle B^0(p)\pi^+(q)|B^{*+}(p+q)\rangle = i(m_\pi^2 - q^2)\int_x e^{iq\cdot x}\langle \bar{B}(p)|\pi(x)|B^*(p+q)\rangle\,. \tag{2.1}$$

Using the PCAC relation

$$\pi(x) = \frac{1}{m_\pi^2 f_\pi}\partial^\mu A_\mu(x)\,, \tag{2.2}$$

where A_μ is, as usual, the QCD axial current, eq. (2.1) becomes

$$\langle B^0(p)\pi^+(q)|B^{*+}(p+q)\rangle = q^\mu \frac{1}{f_\pi}\frac{m_\pi^2 - q^2}{m_\pi^2}\int_x e^{iq\cdot x}\langle \bar{B}(p)|A_\mu(x)|B^*(p+q)\rangle\,. \tag{2.3}$$

The matrix element of the axial current is parametrised in terms of three form factors

$$\begin{aligned}\langle B^0(p)|A_\mu(0)|B^{*+}(p+q)\rangle &= \eta_\mu F_1(q^2) + (\eta\cdot q)\,(2p+q)_\mu F_2(q^2) + \\ &\quad + (\eta\cdot q)\,q_\mu F_3(q^2)\end{aligned} \tag{2.4}$$

yielding for the $B^*B\pi$ coupling

$$g_{B^*B\pi}(q^2) = -\frac{1}{f_\pi}\frac{m_\pi^2 - q^2}{m_\pi^2}\left[F_1(q^2) + \left(m_{B^*}^2 - m_B^2\right)F_2(q^2) + q^2 F_3(q^2)\right]\,. \tag{2.5}$$

In the static limit in which our simulation is performed, the B and B^* mesons are degenerate, so that the form factor F_2 can be discarded.

Analytical continuation of eq. (2.5) towards the soft–pion limit ($q^2 \to 0$), leads to

$$g_{B^*B\pi}(0) = -\frac{1}{f_\pi}F_1(0)\,. \tag{2.6}$$

It is commonly assumed, when deriving the Goldberger-Treiman relation, that $g_{B^*B\pi}$ is a smooth function of q^2, and, therefore, that the physical coupling can be approximated by

$$g_{B^*B\pi} = g_{B^*B\pi}(m_\pi^2) \approx g_{B^*B\pi}(0)\,. \tag{2.7}$$

The above equation explicitly shows that, in the soft–pion limit, the $B^*B\pi$ coupling is related to the form factor of the axial current between B and B^* states. If one were working in the chiral limit from the very beginning, the same Goldberger-Treiman relation, eq. (2.6), would be obtained from the conservation of the axial current.

The relation between $g_{B^*B\pi}$ and g mentioned earlier can be rederived by comparing the matrix element of the Noether current associated to chiral symmetry both in HMχ and QCD. In the chiral limit, the Noether currents associated with chiral symmetry, in QCD and in HMχ, are respectively

$$j^{5\ ab}_{\mathrm{QCD}\ \mu} = \bar{q}^a\gamma_\mu\gamma_5 q^b \tag{2.8}$$

JHEP10(1998)010

Figure 1: Tree-level diagrams needed to compute the matrix element of the axial current in HMχ. The dot ($\bullet$) represents the g-vertex in the HMχ lagrangian; the squares are insertions of the axial current in eq. (2.9).

and

$$j^{5\,ab}_{\mathrm{HM}\chi\;\mu} = f_\pi \partial_\mu \mathcal{M}^{ab} - 2g\left(B^{*\,a\,\dagger}_{\mu} B^b + B^{a\,\dagger} B^{*\,b}_{\mu}\right) + \cdots , \tag{2.9}$$

where the ellipsis denotes terms with more than one pion or terms containing both heavy mesons and pions.

The form factors of the axial current in QCD are related to the coupling of the heavy meson chiral lagrangian by matching the two theories at tree level. The diagrams needed at tree level to evaluate the matrix element in eq. (2.4) for the HMχ current are depicted in fig. 1. A straightforward computation leads to

$$\begin{aligned} F_1(q^2) &= -2g\, m_B \,, \\ F_3(q^2) &= \frac{2g}{q^2} m_B \,, \end{aligned}$$

which, together with the Golberger-Treiman relation, reproduces eq. (1.10). One may also work away from the chiral and heavy quark limits and include corrections for finite mass pions and heavy quarks in this result.

The determination of g is therefore reduced to the computation of the matrix element of the light-light axial vector current between hadronic states. Such an evaluation can be performed using three-point correlation functions on the lattice. The details of the calculation are reported in the next section.

3. Lattice results

3.1. Stochastic propagators

The numerical analysis is carried out on 20 quenched gauge configurations, generated on a $12^3 \times 24$ lattice at $\beta = 5.7$, corresponding to $a^{-1} = 1.10$ GeV. The heavy quark propagators are evaluated in the static limit [18]. Stochastic propagators [19, 20] are used to invert the fermionic matrix for the light quarks. They can be used in place of light quark propagators calculated with the usual deterministic algorithm. The stochastic inversion is based on the relation

$$S_{ij} = M^{-1}_{ij} = \frac{1}{Z}\int \mathcal{D}\phi\; (M_{jk}\phi_k)^* \phi_i\; \exp\left(-\phi^*_i (M^\dagger M)_{ij} \phi_j\right) , \tag{3.1}$$

where, in our case, M is the tadpole improved SW fermionic operator and the indices i, j, k represent simultaneously the space-time coordinates, the spinor and colour indices. Two values of κ are considered, $\kappa_1 = 0.13843$ and $\kappa_2 = 0.14077$, with $c_{\rm sw} = 1.57$. The lighter value κ_2 corresponds to a bare mass of the light quark around the strange mass. The chiral limit corresponds to $\kappa_c = 0.14351$ [21]. For every gauge configuration, an ensemble of 24 independent fields ϕ_i is generated with gaussian probability

$$P[\phi] = \frac{1}{Z} \exp\left(-\phi_i^* (M^\dagger M)_{ij} \phi_j\right) . \tag{3.2}$$

All light propagators are computed as averages over the pseudo-fermionic samples:

$$S_{ij} = \begin{cases} \langle (M\phi)_j^* \phi_i \rangle \\ \text{or} \\ \langle \left(\gamma_5 \phi^*\right)_j \left(M\phi\gamma_5\right)_i \rangle \end{cases} , \tag{3.3}$$

where the two expressions are related by $S = \gamma_5 S^\dagger \gamma_5$. Moreover, the maximal variance reduction method is applied in order to minimise the statistical noise [19]. Maximal variance reduction involves dividing the lattice into two boxes ($0 < t < T/2$ and $T/2 < t < T$) and solving the equation of motion numerically within each box, keeping the spinor field ϕ on the boundary fixed. According to the maximal reduction method, the fields which enter the correlation functions must be either the original fields ϕ or solutions of the equation of motion in disconnected regions. The stochastic propagator is therefore defined from each point in one box to every point in the other box or on the boundary. For this reason, when computing a three-point correlation function

$$\langle 0 | J(t_1, x) \mathcal{O}(t_0, y) J^\dagger(t_2, z) | 0 \rangle , \tag{3.4}$$

one operator — $\mathcal{O}$ in the present work — is forced to be on the boundary ($t_0 = 0$ or $T/2$) and the other two must be in different boxes, while the spatial coordinates are not constrained. If j is a point of the boundary, not all the terms in $(M\phi)_j$ lie on the boundary because the operator M involves first neighbours in all directions. Hence, whenever a propagator S_{ij} is needed with one of the points on the boundary, we use whichever of the two expressions in eq. 3.3 has the spinor $M\phi$ computed away from the boundary.

In smearing the hadronic interpolating operators, spatial fuzzed links are used. Following the prescription in [19, 22], to which the interested reader should refer for details, the fuzzed links are defined iteratively as

$$U_{\rm new} = \mathcal{P}\left(f U_{\rm old} + \sum_{i=1}^{4} U_{{\rm bend},i}\right) , \tag{3.5}$$

where $\mathcal{P}$ is a projector over $SU(3)$ and $U_{{\rm bend},i}$ are the staples attached to the link in the spatial directions. We take $f = 2.5$ and use two iterations with fuzzed links of length one. The smeared fermionic fields are defined following [22].

3.2. Lattice computation

In order to extract g, the three-point correlation function C_3 and the two-point correlation function C_2 for local (L) and fuzzed (F) sources are computed. The FF three-point function is defined as

$$C_{3\ \mu\nu}^{FF}(\mathbf{x};t_1,t_2) = \frac{1}{V}\int d^3y\ \langle 0|J_\nu^{B^*}(\mathbf{y},-t_1)A^\mu(\mathbf{x}+\mathbf{y},0)J^{B\ \dagger}(\mathbf{y},t_2)|0\rangle\,, \tag{3.6}$$

where $J_\nu^{B^*}$ and J^B are fuzzed operators with the quantum numbers corresponding respectively to the B^* and B states. Analogous definitions hold for the FL and LL cases. For time separations that are large enough to isolate the lowest energy states, the three-point function is related to the axial current matrix element:

$$\begin{aligned} C_{3\ \mu\nu}^{FF}(\mathbf{x};t_1,t_2) &\to \langle 0|J_\nu^{B^*}|B_r^*\rangle\frac{\langle B_r^*|A^\mu(\mathbf{x})|B\rangle}{2m_B\,2m_B}\langle B|J^{B\ \dagger}|0\rangle e^{-M_B(t_1+t_2)} = \\ &= Z^F\eta_\nu^r(0)\frac{\langle B_r^*|A^\mu(\mathbf{x})|B\rangle}{2m_B}Z^F e^{-M_B(t_1+t_2)}\,, \end{aligned} \tag{3.7}$$

where r is the polarisation label of the vector particle, and the sum over polarisations is omitted. In the static limit considered in this paper, the slope of the exponential time-decay is not the physical mass of the mesons; it can be interpreted as a binding energy. Moreover, the two-point functions for the vector and pseudoscalar particles are degenerate, leading to the same binding energies and Z factors for both the B and B^*. In order to avoid confusion, the physical mass is denoted by m_B and the binding energy by M_B. Z^F is the overlap of the interpolating operator with the physical state, defined from the two-point functions:

$$\begin{aligned} C_2^{FF}(t) &= \frac{1}{V}\int_V d^3y\ \langle 0|J^B(\mathbf{y},0)J^{B\ \dagger}(\mathbf{y},t)|0\rangle \\ &\to (Z^F)^2 e^{-M_Bt}\,. \end{aligned} \tag{3.8}$$

Integrating the three-point function over $\mathbf{x}$ gives the matrix element for zero momentum transfer. In this limit, the latter can be expressed in terms of the form factor $F_1(q^2)$ in eq. (2.4).

The sum over polarisations in eq. (3.7) yields

$$\int d^3x\ C_{3\ \mu\nu}^{FF}(\mathbf{x};t_1,t_2) \to (Z^F)^2(g_{\mu\nu} - \frac{p_\mu p_\nu}{m_B^2})F_1(0)e^{-M_B(t_1+t_2)}\,. \tag{3.9}$$

The last equation shows that the three-point functions with $\mu \neq \nu$ and $\mu = \nu = 0$ should vanish. Therefore, only the correlators with $\mu = \nu = 1,2,3$ are henceforth considered.

Moreover, taking rotational symmetry into account, $C_3^{FF}(\mathbf{x};t_1,t_2)$ is expected to be a function of the distance r only, up to cut-off effects. The three-point functions measured on the lattice are averaged over equivalent $\mathbf{x}$ positions.[2] The desired matrix element is obtained from the ratio

$$E_\mu(r,t) \stackrel{\text{def}}{=} (Z^F)^2 \overline{\sum_r}^x \frac{C_{3\ \mu\mu}^{FF}(\mathbf{x},t,t)}{C_2^{FF}(t) C_2^{FF}(t)} \to \frac{\langle B^* | A_\mu(r) | B \rangle}{2 m_B} \eta_\mu \,, \tag{3.10}$$

where the time-dependence cancels when the three-point function is divided by the product of two-point functions.

The coefficients Z^F and Z^L are extracted from the exponential fit of the two point correlation functions C_2. The data are reported in fig. 2. As one can see from the plots, the two-point functions already exhibit a single-exponential behaviour at moderate time separations. The main sources of error in this computation are expected to stem from the determination of the three-point function and from the value of the light quark masses, which are far from the chiral limit. Thus, a single exponential fit of the two-point functions turns out to be accurate enough for the scope of this study. The value of Z^F is extracted from a direct fit of C_2^{FF}, while Z^L is obtained from C_2^{FF} and C_2^{FL}. The results of the fit are shown directly on the plot. It is worth remarking that, in all the channels considered, single-exponential fits yield reasonable values for the reduced χ^2.

The B meson decay constant, in the static approximation, can be extracted from:

$$f_B^{\text{static}} = Z_A^{\text{static}} \sqrt{\frac{2}{m_B}} Z^L a^{-3/2} \,, \tag{3.11}$$

where Z_A^{static} is the renormalisation constant for the axial current in the static theory, which is discussed in the following section and defined in eq. (4.11). The aim here is not a precise determination of the pseudoscalar decay constant, f_B^{static}. Rather, the result is presented to allow an estimate of the systematic errors in our computation of the HMχ coupling, g.

The results of the fits, together with the values for f_B^{static} are summarised in tab. 1. The B meson binding energies obtained from the fits of C_2^{FF} and C_2^{FL} are consistent with each other. However, our determination appears to be slightly different from the

[2]The symbol

$$\overline{\sum_r}^x$$

indicates the average on all the spatial positions on the lattice compatible with the constraint $|x| = r$. On a finite lattice $V = L^3$, only some distances are allowed

$$r = \sqrt{x_1^2 + x_2^2 + x_3^2}$$

because each x_i must be an integer between 0 and L/2. For each allowed distance r, a given number of terms N_r appears in the above sum, yielding a relative error on each point $\delta E_\mu(r,t) \sim N_r^{-1/2}$, e.g.

$$N_0 = 1;\ N_1 = 6;\ N_{\sqrt{2}} = 12;\ N_{\sqrt{3}} = 6;\ \ldots;\ N_{\sqrt{108}} = 1$$

.

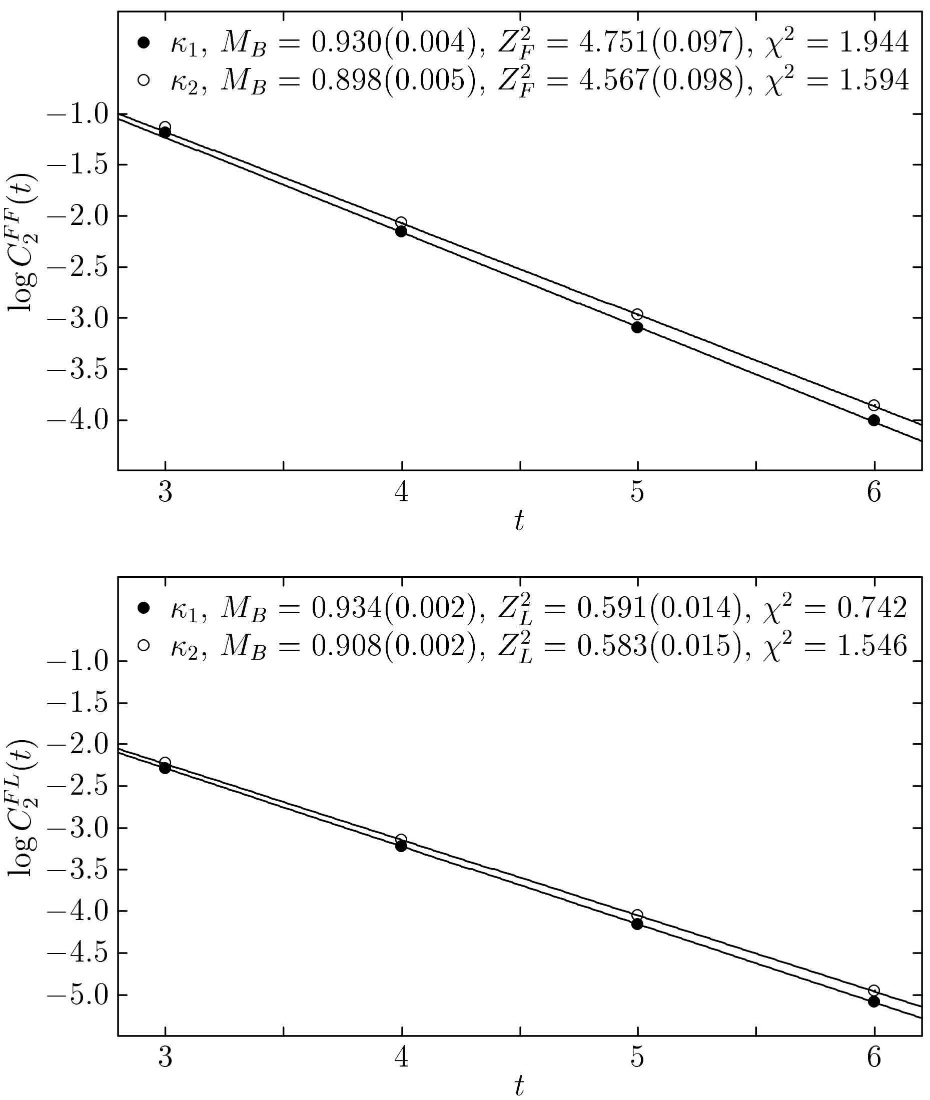

Figure 2: Logarithmic plots of $C_2^{FF}(t)$ and $C_2^{FL}(t)$ for both values of κ. The quoted values refer to the reduced χ^2.

one published in [19]. The discrepancy can be explained as a contribution from excited states, which is subtracted in [19] where a multi-exponential fit is performed. The 1-state fit yields a value of Z^L approximately 20% higher than the one obtained from the 3-state fit. Hence the value obtained for the static B decay constant lies above other lattice calculations of this quantity [17]. It is striking that the actual number does not depend on the value of the hopping parameter κ. However the variation, as the bare mass of the quark goes from m_s towards the chiral limit, is also expected to be about 20% and could be obscured by the contamination from excited states.

This is a first, exploratory, direct lattice determination of the coupling g, so the discrepancies noted above are perhaps expected and could easily arise from various lattice artefacts. Our value of β is far from the continuum limit, while our action and operators are not fully $O(a)$ improved. We have not tried to optimise the smearing or

	κ_1	κ_2	κ_c
$M_B a$	0.930(4)	0.898(5)	0.862(7)
$(Z^F)^2$	4.75(10)	4.57(10)	4.37(15)
$(Z^L)^2$	0.59(1)	0.58(2)	0.57(3)
f_B^{static}(GeV)	0.43(1)	0.43(1)	0.42(2)

Table 1: Values for Z^F, Z^L, M_B and f_B^{static} obtained from fitting the two-point functions.

fitting procedures. Our ensemble of gauge configurations and the collection of spinor configurations on each gauge sample are quite small. The calculation is also performed in the quenched approximation. All of these issues could be addressed in a further simulation, but here we will keep in mind that the uncertainties will propagate as systematic errors to our final result for the $B^*B\pi$ coupling.

The generation of stochastic propagators for the light quark and the static approximation for the heavy quark have proved to be useful tools in this investigation. However, neither is strictly necessary to calculate the axial current matrix element of interest. One could combine static heavy quarks with light quark propagators determined by standard deterministic methods. A full $O(a)$-improved simulation with heavy quark masses around the charm mass would allow one to go beyond the static approximation and study the dependence of g on the heavy mass. The freedom allowed in lattice calculations to tune quark masses would also allow the light quark mass dependence, noted above as strikingly absent, to be investigated in more detail.

Returning to the results of the present simulation, the quantity $E_0(x,t)$, which is expected to vanish, is measured as a further consistency check. The data reported in figs. 3 and 4 show a much smaller signal than the one obtained for $E_i(x,t)$. As t is increased, the fictitious peak at zero distance decreases, while the noise increases.

Using rotational invariance, the average of the three spatial components of $E_i(r,t)$

$$\overline{E}(r,t) = \frac{1}{3}(E_1(r,t) + E_2(r,t) + E_3(r,t)) \tag{3.12}$$

is measured. The results are reported in figs. 3 and 4, for the two values of κ used in this simulation. At fixed r, $\overline{E}(r,t)$ is expected to be independent of t. As this behaviour is confirmed by the data, the signal can be improved by averaging the values at different times, each weighted with its error, yielding a function of the spatial distance $\overline{E}(r)$, which needs to be integrated over the three-dimensional volume. Since this is an exploratory calculation we have neglected the effects of correlations between neighbouring time slices on the error in the average, which would increase the statistical error in our result. However, we note that the systematic errors considered below in any case dominate the uncertainty in the values at each time. The time-slices considered in the average are $t = 4, 5, 6$. Logarithmic plots of $\overline{E}(r)$ is displayed in figs. 5 and 6 for both values of κ, suggesting that the data are consistent with an exponential decay.

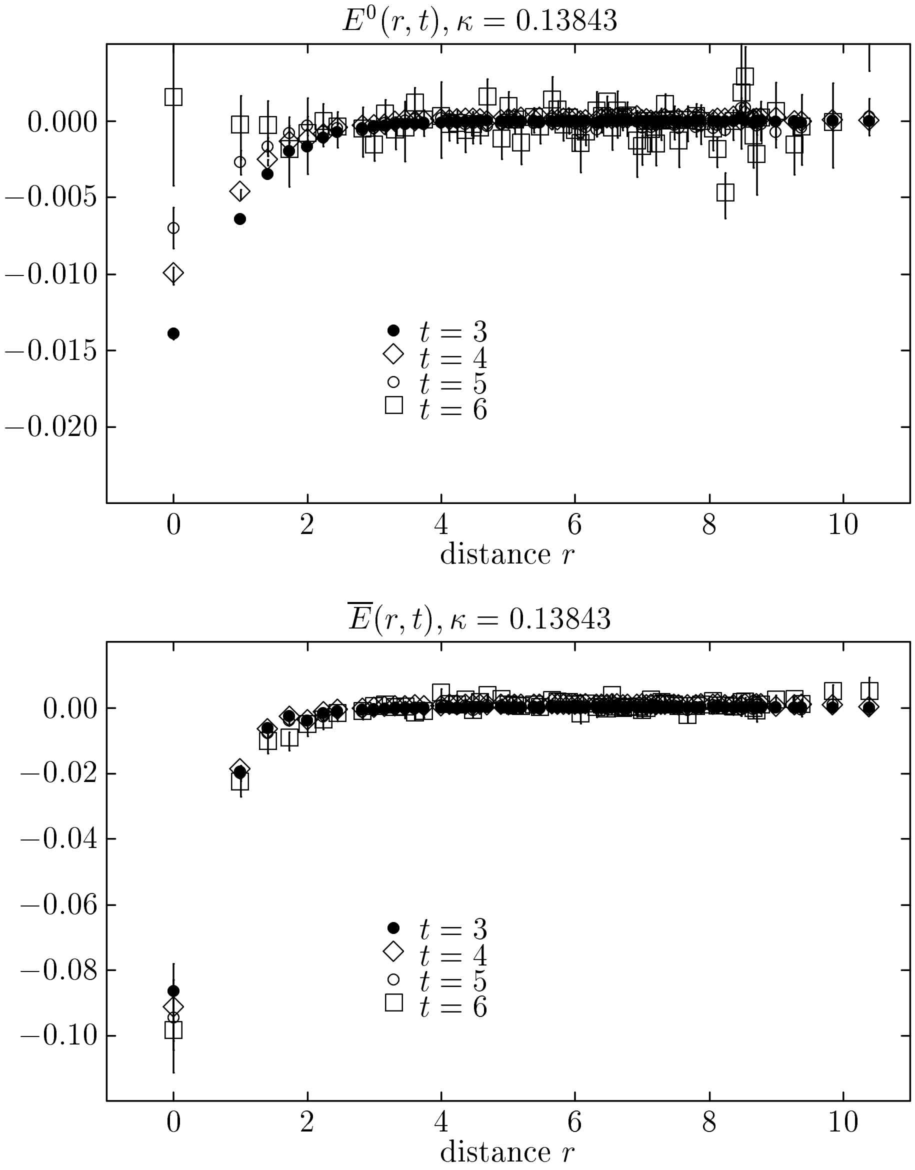

Figure 3: Plots of $E^0(r,t)$ and $\overline{E}(r,t)$ as functions of r for different values of t $(= 3, 4, 5, 6)$ for $\kappa = 0.13843$.

To evaluate the volume integral, $\overline{E}(r)$ is fitted with a two-parameter exponential for each value of κ,

$$f(r) = Se^{-r/r_0}\,. \tag{3.13}$$

The results of the fit and the values of the reduced χ^2 are recorded on the figures. The coupling g is finally obtained by integrating analytically the fitted function:

$$g^{\mathrm{L}} = -\int_0^\infty 4\pi r^2 \overline{E}(r) dr = -\int_0^\infty 4\pi r^2 f(r) dr\,. \tag{3.14}$$

The superscript L indicates that these numbers are defined on the lattice using operators renormalised at the lattice energy scale $a^{-1} = 1.10$ GeV. As for the two-point functions, the value of g^{L} does not appear to depend on the mass of quarks. It is not

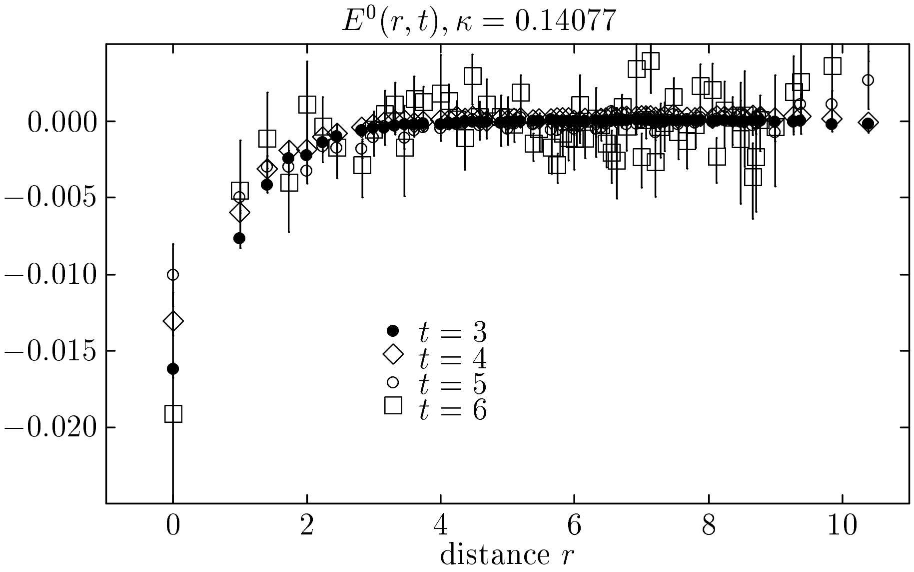

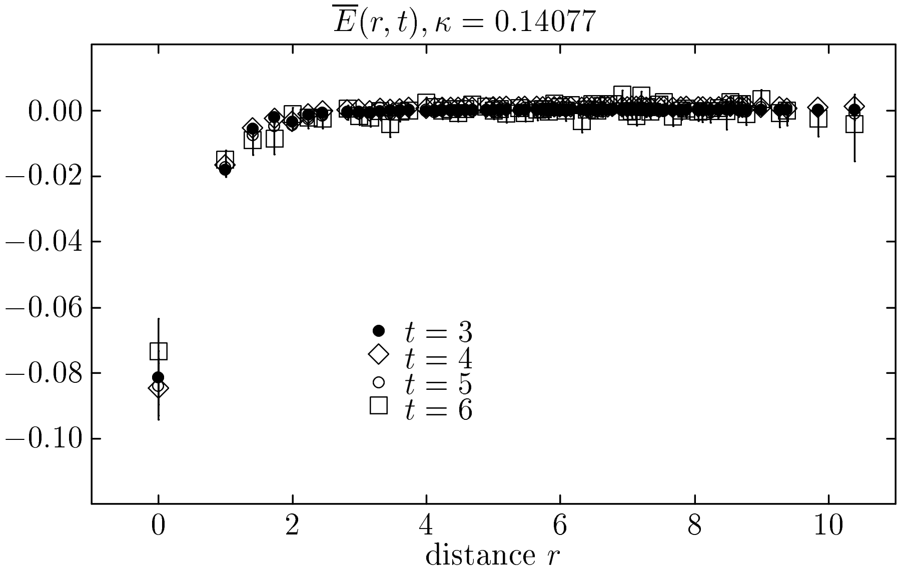

Figure 4: Plots of $E^0(r,t)$ and $\overline{E}(r,t)$ as functions of r for different values of t $(= 3, 4, 5, 6)$ for $\kappa = 0.14077$.

clear from this simulation, whether this is a genuine physical feature or, as explained earlier, an artefact of the lattice used here. Further studies should aim to clarify this point.

The best estimate for g^{L} at $\kappa = \kappa_c$ is thus obtained from a weighted average of the results at the two kappas used in our simulations:

$$g^{\mathrm{L}} = 0.52(5)(10)\,. \tag{3.15}$$

The first error is statistical; the second is a conservative estimate of the systematic error of 20%, based on the systematic error observed in the estimate of f_B.

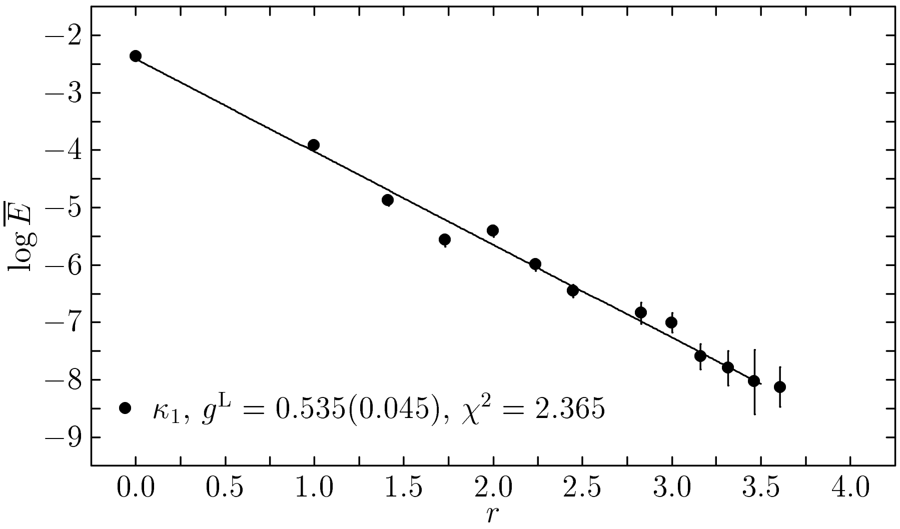

Figure 5: Plot of $\overline{E}(r)$ as a function of r for $\kappa = 0.13843$.

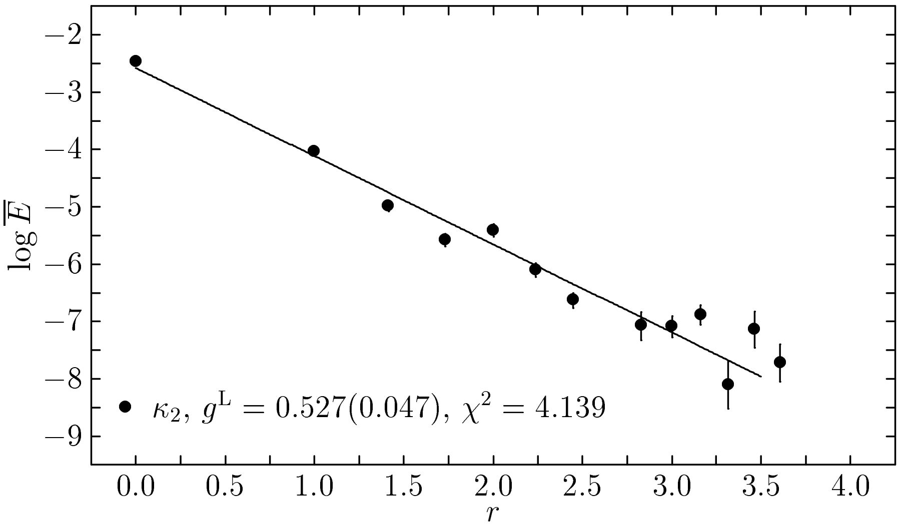

Figure 6: Plot of $\overline{E}(r)$ as a function of r for $\kappa = 0.14077$.

4. Renormalisation constants

Quantities evaluated on the lattice are connected to their continuum counterparts by a finite renormalisation. In order to extract physical information, the matrix element of a bilinear quark operator defined on the lattice, $\mathcal{O}^{\rm L}(a)$, has to be multiplied by the corresponding renormalisation constant

$$\mathcal{O}(\mu) = Z_{\mathcal{O}}(a\mu, g)\ \mathcal{O}^{\rm L}(a)\,. \tag{4.1}$$

which in general depends on the renormalisation scale μ and the details of the lattice discretization (a single continuum operator may also match onto a set of lattice operators). For partially conserved currents, the μ dependence disappears in the above definition, the associated anomalous dimension being equal to zero. This is the case for the QCD light-light axial current considered here. It is also the case for the heavy-light current in full QCD, but not for the static-light current onto which it matches in the effective theory: hence the renormalisation constant $Z_A^{\rm static}$ in eq. (4.11) below, which converts the lattice matrix element to the physical $f_B^{\rm static}$, includes the effect of running between different scales in the effective theory.

In our simulation, we use the standard gluon action and the tadpole-improved [23] Sheikholeslami-Wohlert [24] fermion action for the light quarks:

$$
\begin{aligned}
S = \frac{a^4}{2\kappa}\sum_{xy}\bar\psi(x)\Big\{&\Big[1-\frac{i\tilde\kappa a}{2u_0^4}\sigma_{\mu\nu}F_{\mu\nu}(x)\Big]\delta_{xy} \\
&-\frac{\tilde\kappa}{au_0}\Big[(1-\gamma_\mu)U_\mu(x)\delta_{x+\hat\mu,y}+(1+\gamma_\mu)U_\mu^\dagger(y)\delta_{x-\hat\mu,y}\Big]\Big\}\psi(y)\,,
\end{aligned}
\tag{4.2}
$$

where as usual $F_{\mu\nu}(x)$ is a lattice definition of the gluon field strength tensor, $\tilde\kappa=\kappa u_0$ and we define u_0 from the average plaquette in infinite volume, $u_0^4=\langle\frac{1}{3}\,{\rm Tr}\,U_\Box\rangle$. The redefinition of the parameters in the action is done in order to absorb the large renormalisation coming from lattice tadpole graphs [23]. The standard definition of $c_{\rm sw}$, the coefficient of the $\sigma_{\mu\nu}F_{\mu\nu}$ term, in this case gives $c_{\rm sw}=1/u_0^3$. For our lattice, $u_0=0.86081$ from the average plaquette, so that $c_{\rm sw}=1.57$. For the b quarks we use the standard static quark action. Here we summarise the required renormalisation constants for the light-light and static-light axial currents with the action and parameters defined above.

The matrix element of the light-light axial current between an initial state i and a final state f in the continuum can be written as:

$$
\langle f|A_\mu|i\rangle = Z_A\langle f|A_\mu^{\rm L}|i\rangle = Z_A^{\rm 1-loop}\frac{u_0}{u_0^{\rm 1-loop}}\langle f|A_\mu^{\rm L}|i\rangle\,. \tag{4.3}
$$

The factor u_0, a measure of the average link variable, can be interpreted as a non-perturbative rescaling of the quark fields in the tadpole improvement prescription. The 1-loop perturbative renormalisation constant must then be redefined by dividing out the 1-loop expression, $u_0^{\rm 1-loop}$, corresponding to the chosen definition of u_0,

$$
Z_A^{\rm tadpole} = Z_A^{\rm 1-loop}/u_0^{\rm 1-loop}\,. \tag{4.4}
$$

The overall renormalisation constant is given by the whole factor

$$
Z_A = u_0\,Z_A^{\rm tadpole}\,. \tag{4.5}
$$

The perturbative part reads

$$
\frac{Z_A^{\rm 1-loop}}{u_0^{\rm 1-loop}} = \frac{1+\frac{\alpha C_F}{4\pi}\zeta_A}{1+\frac{\alpha C_F}{4\pi}\lambda} \simeq 1+\frac{\alpha C_F}{4\pi}(\zeta_A-\lambda)\,, \tag{4.6}
$$

where $\lambda=-\pi^2$ for our plaquette definition of u_0 and $\zeta_A=-13.8$ [26, 27, 28].

We note here that the removal of tree-level $O(a)$ discretisation errors is achieved by combining the Sheikholeslami-Wohlert action for $c_{\rm sw} = 1$ with improved operators, found by redefining or "rotating" the quark fields [29]. In our simulation, the rotation has not been applied to the quarks, so the perturbative coefficient ζ above is calculated using the improved action only. Moreover, in perturbation theory, $c_{\rm sw} = 1 + O(\alpha)$, so we quote ζ above calculated for $c_{\rm sw} = 1$, without rotated light quark fields. In [30] the light fermion bilinear operator renormalisations are given as functions of $c_{\rm sw}$ and an arbitrary amount of field rotation: using our actual value of $c_{\rm sw} = 1.57$, with no field rotation, in those results would increase Z_A by 5%.

The mean-field improved perturbative expansion is performed in terms of a boosted coupling constant, $\tilde{\alpha}$, which in our case is chosen as $\tilde{\alpha} = \alpha_0/u_0^4$, where α_0 is the bare lattice coupling constant. We use $\tilde{\alpha}$ for α in eq. (4.6). For our lattice, with $\beta = 5.7$ and $u_0 = 0.86081$ from the average plaquette, this leads to

$$Z_A = u_0\, Z_A^{\rm tadpole} = 0.806\,. \tag{4.7}$$

For the heavy-light axial current computed in the static limit, the renormalisation constant $Z_A^{\rm static}$ is found by a three step procedure combining the matching between full QCD and the continuum static theory at a scale of order m_b [31], the continuum static theory running from m_b to a lattice scale q^* [32, 33, 34] and finally the matching between the continuum static and the lattice static theories [35, 36]. Since we have performed a quenched lattice simulation we encounter the standard problem of matching a zero-flavour result to a continuum result with active flavours. We adopt a standard procedure of matching quenched to continuum results at q^* and then performing the continuum running with the appropriate number of flavours.[3] We extract from the calculation of Borrelli and Pittori [36] the appropriate matching factor corresponding to our case of an improved action, but without field rotations on the light quarks. In the notation of [36] the number we need is

$$C_F(5/4 - A_{\gamma_0\gamma_5} - d^I - f^I/2 + (e - e^{\rm red})/2) = -19.21\,. \tag{4.8}$$

This appears in eq. (4.11) below and contrasts with the values -27.2 for the Wilson action and -20.0 for the improved action with $c_{\rm sw} = 1$ and field rotations included (We have recomputed the numerical integrals so these values differ in the last two figures from those quoted in [36]. The difference is, however, less than 1%).

In the matching to the lattice we will adopt a Lepage-Mackenzie choice [23] of the scale q^* at which to perform the matching. This scale is determined from the expectation value of $\ln(qa)^2$ in the one-loop lattice perturbation theory integrals for the corrections to the renormalisation constant, including the perturbative tadpole

[3] One could decide to match the lattice to the continuum result at a different scale, then perform the continuum running with the appropriate number of flavours from that scale to m_b. However, for any choice of the intermediate scale between q^* and m_b, the difference in the final result is of the order of 2%, which is negligible compared to the systematic error due to the quenched approximation.

JHEP10(1998)010

improvement corrections for the chosen definition of u_0. For the improved, $c_{\rm sw} = 1$, ation and plaquette definition of u_0, Giménez and Reyes [37] quote $q^*a = 2.29$. We will use this value.

We will also adopt a plaquette definition of the lattice coupling constant according to (for zero flavours):

$$-\ln(\langle \mathrm{Tr}\, U_\square \rangle/3) = \frac{4\pi}{3}\alpha_V(3.41/a)(1 - 1.19\alpha_V)\,. \tag{4.9}$$

Once $\alpha_V(3.41/a)$ is determined, we can use the equation for the running of α_V,

$$\alpha_V(q) = \frac{4\pi}{2b_0 \ln(q/\Lambda_V) + b_1 \ln\left(2\ln(q/\Lambda_V)\right)/b_0} \tag{4.10}$$

to determine $\alpha_V(q^*)$. In the quenched theory, $b_0 = 11$ and $b_1 = 102$. We find $a\Lambda_V = 0.294$ and $\alpha_V(q^*) = 0.216$.

Since $q^* = 2.52\,\mathrm{GeV}$ is between the charm and b quark thresholds we perform the continuum running with four active flavours. From the Particle Data Group (PDG) [38], we take $\Lambda^{(5)}_{\overline{\rm MS}} = 237^{+26}_{-24}\,\mathrm{MeV}$ using two-loop running, and find $\Lambda^{(4)}_{\overline{\rm MS}}$ using continuity of the strong coupling at the b quark threshold. This threshold value is given by m_b satisfying $m_{b\,\overline{\rm MS}}(m_b) = m_b$. We take $m_b = 4.25\,\mathrm{GeV}$, using the average of the range, 4.1–4.4 GeV, quoted by the PDG [38].

The overall renormalisation constant is thus given by:

$$\begin{aligned} Z_A^{\rm static} &= \left(\frac{\alpha(m_b)}{\alpha(q^*)}\right)^d \left\{1 - c\frac{\alpha(m_b)}{4\pi} + \frac{\alpha(q^*)-\alpha(m_b)}{4\pi}J_A\right\} \times \\ &\quad \times \sqrt{u_0}\left(1 + \frac{\alpha_V(q^*)}{4\pi}[4\ln(q^*a) - 19.36 - C_F\lambda/2]\right), \end{aligned} \tag{4.11}$$

where $c = 8/3$, $J_A = 0.91$ and $d = -6/25$. Using the inputs given above, we find

$$Z_A^{\rm static} = 0.78\,. \tag{4.12}$$

Independent variations of $\Lambda^{(5)}$ and m_b to the ends of the ranges quoted above and $\pm 10\%$ variation in a^{-1} change this value by 1.3% or less. Changing q^* to $1/a$ or π/a reduces $Z_A^{\rm static}$ by 13% or raises it by 1.3% respectively.

We close this section by noting that both Z_A and $Z_A^{\rm static}$ are evaluated in the chiral limit and so do not depend on the light quark mass used in the simulation.

5. Phenomenological implications

We now combine the lattice matrix element with its renormalisation factor to find the continuum value for g. Since we observe no light quark mass dependence in g^L and evaluated the renormalisation constant in the chiral limit, we multiply the lattice matrix element in eq. (3.15) by the renormalisation constant in eq. (4.7), to obtain:

$$g = Z_A\, g^{\rm L} = 0.42(4)(8) \tag{5.1}$$

for the coupling of the heavy mesons with the Goldstone bosons.

Reference	g	Reference	g
[6]	0.32(2)	[41]	0.7
[42]	0.39	[5]	0.75-1.0
[3][a]	0.44 (16)	[43, 44]	0.4-0.7
		[45]	0.38

[a]Combined sum rule + lattice results

Table 2: Recent determinations of the coupling constant g

The direct decay $B^* \to B\pi$ is kinematically forbidden. However, the corresponding reaction occurs in the D system, where the coupling $g_{D^*D\pi}$ is also related to g by an expression analogous to eq. (1.10), although the $1/m_Q$ corrections are expected to be larger in the charm case. A recent analysis [39], incorporating chiral symmetry breaking corrections plus $1/m_c$ corrections in the HMχ lagrangian and fitting to the branching ratios for $D^{*0} \to D^0\pi^0$, $D^{*+} \to D^+\pi^0$ and $D_s^* \to D_s\pi^0$ (together with radiative decay rates for the same D^* mesons), gives

$$g = \begin{cases} 0.27(^{4}_{2})(^{5}_{2}) \\ 0.76(3)(^{2}_{1}) \end{cases} . \tag{5.2}$$

The two fold ambiguity can be resolved by imposing the experimental limit $\Gamma(D^{*+}) < 0.13\,\mathrm{MeV}$ [40], which gives $g < 0.52$ to a good approximation [39].

Other estimates of g are derived using constituent quark models and sum rules. Starting from the non-relativistic result $g = 1$, quark models can be improved using more sophisticated assumptions to describe the quark dynamics inside the meson. Independent estimates are obtained from computing QCD correlation functions in the framework of sum rules. To give an idea of the range spanned by different determinations, some recent results are listed in tab. 2, while our value together with the average of other determinations is displayed in fig. 7.

The best estimate from a global analysis of available results, quoted in the review [3], is

$$g \simeq 0.38 \tag{5.3}$$

with a total uncertainty of 20%; the latter being comparable with the estimated systematic error from our lattice computation. Not only is the result presented in this paper compatible with the previous estimates; the systematic error is also competitive when compared to the above results.

The agreement with other previous estimates is pleasing, but the value of the coupling g can also be used to check the consistency of the heavy quark symmetry predictions in the soft pion limit for the lattice results.

The form factor f_1 of the semileptonic decay $B \to \pi l\nu$ is predicted to have the expression given earlier in eq. (1.12). This behaviour for $f_1(q^2)$ is expected to be valid near zero recoil ($q^2 \to q^2_{\max}$), where the closest vector resonance dominates, even beyond

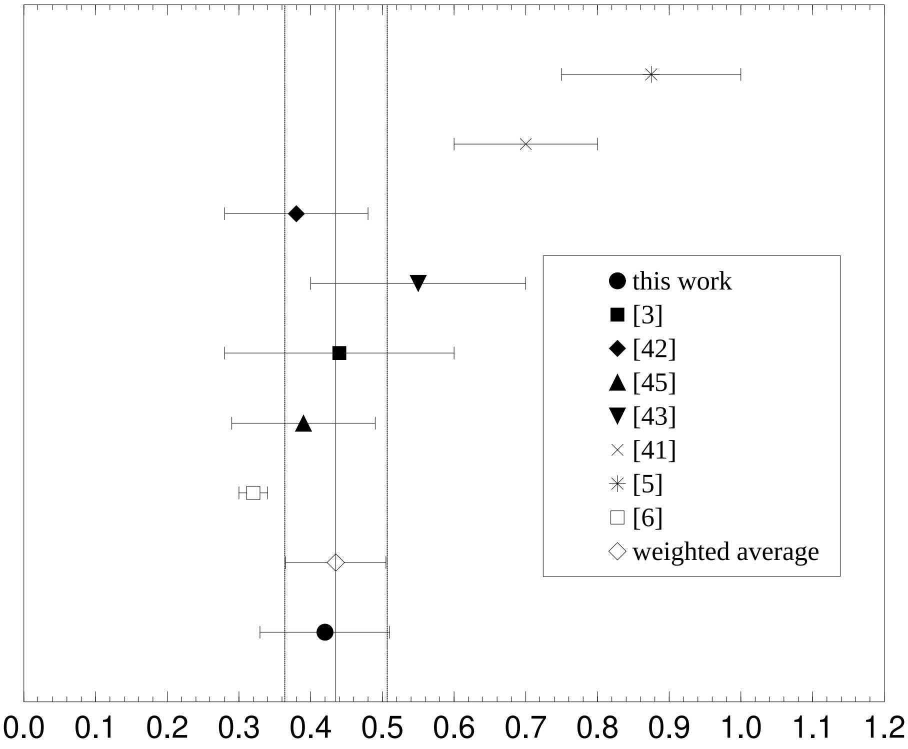

Figure 7: Comparison of various estimates of the coupling g.

the leading approximation in $1/m_b$ in HQET [11]. One also obtains this behaviour from the heavy meson chiral lagrangian [1, 7, 8, 9], valid for a low momentum pion. It is perhaps surprising that such a behaviour is found by sum rules to hold reasonably, at least for the D meson, also at $q^2 \to 0$ [6]. In this case the coupling g would fix the normalisation of the form factor f_1 . The extension of the validity of the vector pole dominance for general values of q^2 has no simple theoretical justification. It can be argued that the contributions from different resonances can lead to a single pole behaviour; however, in this case, the relation between g and $f_1(0)$ would be spoilt.

Lattice data for the semi-leptonic B decay form factors have been fitted assuming a pole behaviour for f_1 [14], yielding $f_1(0) = 0.44(3)$, to be compared with

$$f_1(0)|_{\mathrm{VMD}} = \frac{m_B}{f_\pi f_{B^*}} g \tag{5.4}$$

from eq. (1.12). Our determination of g gives $f_1(0) = 0.50(5)(10)$, in good agreement with the direct fit. Such an agreement should not come as a surprise: the lattice data, after chiral extrapolation, turn out to be close to the end-point of the phase space kinematically allowed for $B \to \pi$ decays ($q^2 \simeq q^2_{max}$). The lattice normalisation of the form factor comes therefore from a fit in a region where vector dominance does hold. Hence, the above agreement should be seen as a consistency check of the two lattice computations. It is nevertheless important to see that the two results are not contradictory.

Assuming a pole form for f_1, an independent bound on the value of the residue is obtained by enforcing the theory to satisfy unitarity [46]. The bound quoted in [46] is

$$f_1(0) m_{B^*}^2 \leq 10\,\mathrm{GeV}^2\,, \tag{5.5}$$

which translates into

$$f_1(0) \leq 0.4\,. \tag{5.6}$$

This, again, agrees reasonably with the determination obtained from VMD, using our value for g, and the one coming from the direct fit of the lattice form factors.

As the lattice determinations will improve in the future, the comparison of the three results summarised here could become an effective way to constrain the residue at the B^* pole.

6. Conclusions

We have shown that the coupling $g_{B^*B\pi}$, or equivalently the coupling g in the HMχ lagrangian, may be evaluated on the lattice from the matrix element of the light quark axial current between B and B^* states. The value of g enters many phenomenological quantities of interest calculated in heavy meson chiral perturbation theory, including the form factors for semileptonic $B \to \pi$ decays mentioned here, as well as $B^* \to \pi$ decays and other quantities such as ratios of heavy meson nonleptonic decay constants, heavy meson mass splittings and radiative decays.

Even the relatively crude estimate obtained here should be interesting for heavy meson phenomenology, but we believe future more precise lattice computations would be valuable.

Acknowledgments

It is a pleasure to acknowledge enlightening discussions with C.T. Sachrajda. We would also like to thank L. Lellouch, R. Petronzio, G.C. Rossi and H. Wittig for discussing some of the issues presented here.

Numerical simulations were performed on a CRAY J90 computer at RAL, under grant GR/L55056. GdD is supported by a University of Southampton Annual Grant Award, LDD, JMF, GdD and MDP by PPARC under grants GR/L56329 and GR/L29927, and by EPSRC grant GR/K41663. JMF thanks the CERN Theory Division for hospitality during the completion of this work.

References

[1] M.B. Wise, *Phys. Rev.* **D 45** (1992) 2188.

[2] B. Grinstein, *An Introduction to Heavy Mesons*, 6th Mexican School of Particles and Fields, Villahermosa, Tabasco, October 1994, University of California San Diego preprint UCSD–PTH–95–05, `hep-ph/9508227`.

[3] R. Casalbuoni, A. Deandrea, N. Di Bartolomeo, R. Gatto, F. Feruglio and G. Nardulli, *Phys. Rep.* **281** (1997) 145 [hep-ph/9605342] and references therein.

[4] M. Neubert, *Phys. Rep.* **245** (1994) 259 [hep-ph/9306320].

[5] T.-M. Yan, H.-Y. Cheng, C.-Y. Cheung, G.-L. Lin, Y.C. Lin and H.-L. Yu, *Phys. Rev.* **D 46** (1992) 1148.

[6] V.M. Belyaev, V.M. Braun, A. Khodjamirian and R. Rückl, *Phys. Rev.* **D 51** (1995) 6177 [hep-ph/9410280].

[7] H.-Y. Cheng et al., *Phys. Rev.* **D 49** (1994) 2490 [hep-ph/9308283].

[8] R. Fleischer, *Phys. Lett.* **B 303** (1993) 147.

[9] A.F. Falk and B. Grinstein, *Nucl. Phys.* **B 416** (1994) 771 [hep-ph/9306310].

[10] C.G. Boyd and B. Grinstein, *Nucl. Phys.* **B 442** (1995) 205 [hep-ph/9402340].

[11] G. Burdman, Z. Ligeti, M. Neubert and Y. Nir, *Phys. Rev.* **D 49** (1994) 2331 [hep-ph/9309272].

[12] For a review, see: V.M. Braun, *Light-cone sum rules*, to appear in Proc. 4th Int. Workshop on Progress in Heavy Quark Physics, Rostock, Germany, September 1997, hep-ph/9801222.

[13] A. Khodjamirian, R. Rückl and C.W. Winhart, *Phys. Rev.* **D 58** (1998) 054013 [hep-ph/9802412].

[14] UKQCD Collaboration, L. Del Debbio, J.M. Flynn, L. Lellouch and J. Nieves, *Phys. Lett.* **B 416** (1998) 392 [hep-lat/9708008].

[15] L. Lellouch, *Nucl. Phys.* **B 479** (1996) 353 [hep-ph/9509358].

[16] P. Ball and V.M. Braun, *Phys. Rev.* **D 55** (1997) 5561 [hep-ph/9701238];
V.M. Belyaev, A. Khodjamirian and R. Rückl, *Z. Physik* **C 60** (1993) 349 [hep-ph/9305348].

[17] H. Wittig, *Int. J. Mod. Phys.* **A 12** (1997) 4477 [hep-lat/9705034].

[18] E. Eichten, *Nucl. Phys.* **4** *(Proc. Suppl.)* (1988) 147 [hep-ph/9801258];
E. Eichten and B. Hill, *Phys. Lett.* **B 232** (1989) 113.

[19] UKQCD Collaboration, C. Michael and J. Peisa, University of Liverpool preprint LTH-420, *Phys. Rev.* **D 58** (1998) 034506 [hep-lat/9802015].

[20] G.M. de Divitiis, R. Frezzotti, M. Masetti and R. Petronzio, *Phys. Lett.* **B 382** (1996) 393 [hep-lat/9603020].

[21] UKQCD Collaboration, H. Shanahan et al., *Phys. Rev.* **D 55** (1997) 1548 [hep-lat/9608063].

[22] UKQCD Collaboration, P. Lacock, A. McKerrell, C. Michael, I.M. Stopher and P.W. Stephenson, *Phys. Rev.* **D 51** (1995) 6403 [hep-lat/9412079]

[23] G.P. Lepage and P.B. Mackenzie, *Phys. Rev.* **D 48** (1993) 225.

[24] B. Sheikholeslami and R. Wohlert, *Nucl. Phys.* **B 259** (1985) 572.

[25] UKQCD Collaboration, A.K. Ewing et al., *Phys. Rev.* **D 54** (1996) 3526 [hep-lat/9508030].

[26] C.T. Sachrajda, private communication.

[27] M. Lüscher, S. Sint, R. Sommer and H. Wittig, *Nucl. Phys.* **B 491** (1997) 344 [hep-lat/9611015].

[28] E. Gabrielli, G. Martinelli, C. Pittori, G. Heatlie and C.T. Sachrajda, *Nucl. Phys.* **B 362** (1991) 475.

[29] G. Heatlie et al., *Nucl. Phys.* **B 352** (1991) 266.

[30] M. Göckeler et al., Proceedings Lattice 96: 14th International Symposium on Lattice Field Theory, St. Louis, June 1996, *Nucl. Phys.* **53** *(Proc. Suppl.)* (1997) 896 [hep-lat/9608033].

[31] E. Eichten and B. Hill, *Phys. Lett.* **B 234** (1990) 511.

[32] X. Ji and M.J. Musolf, *Phys. Lett.* **B 257** (1991) 409.

[33] D.J. Broadhurst and A.G. Grozin, *Phys. Lett.* **B 267** (1991) 105; *ibid.* **274** (1991) 421.

[34] V. Giménez, *Nucl. Phys.* **B 375** (1992) 582.

[35] E. Eichten and B. Hill, *Phys. Lett.* **B 240** (1990) 193.

[36] A. Borrelli and C. Pittori, *Nucl. Phys.* **B 385** (1992) 502.

[37] V. Giménez and J. Reyes, IFIC Valencia preprint, FTUV 98/2, IFIC 98/2, hep-lat/9806023.

[38] Particle Data Group, C. Caso et al., *Euro. Phys. J.* **C 3** (1998) 1.

[39] I.W. Stewart, *Nucl. Phys.* **B 529** (1998) 62 [hep-ph/9803227 v2].

[40] ACCMOR Collaboration, S. Barlag et al., *Phys. Lett.* **B 278** (1992) 480.

[41] S. Nussinov and W. Wetzel, *Phys. Rev.* **D 36** (1987) 130.

[42] P. Colangelo, G. Nardulli, A. Deandrea, N. Di Bartolomeo, R. Gatto and F. Feruglio, *Phys. Lett.* **B 339** (1994) 151 [hep-ph/9406295].

[43] P. Cho and H. Georgi, *Phys. Lett.* **B 296** (1992) 408 [hep-ph/9209239].

[44] J.F. Amundson et al., *Phys. Lett.* **B 296** (1992) 415 [hep-ph/9209241].

JHEP10(1998)010

[45] P. Colangelo, F. De Fazio and G. Nardulli, *Phys. Lett.* **B 334** (1994) 175 [hep-ph/9406320].

[46] C.G. Boyd, B. Grinstein and R.F. Lebed, *Phys. Rev. Lett.* **74** (1995) 4603 [hep-ph/9412324]. This paper uses a different convention to us for the vector decay constant, f_{B^*}, and their $g_{B^*B\pi}$ is half as big as ours.

JHEP10(1998)010